International Journal of Nanomedicine

Dovepress

open access to scientific and medical research

Open Access Full Text Article

ORIGINAL RESEARCH

Eco-Friendly Synthesis of MnO_2 Nanorods Using *Gmelina arborea* Fruit Extract and Its Anticancer Potency Against MCF-7 Breast Cancer Cell Line

Chandrashekar Srinivasa[1,*], SR Santosh Kumar[2], Sushma Pradeep[3], Shashanka K Prasad[3], Ravindra Veerapur[4], Mohammad Azam Ansari[5], Mohammad N Alomary[6], Saad Alghamdi[7], Mazen Almehmadi[8], Kavitha GC[1], Azharuddin B Daphedar[9], Siddappa B Kakkalameli[10], Chandan Shivamallu[3,*], Shiva Prasad Kollur[11,12,*]

[1]Department of Studies in Biotechnology, Davangere University, Davangere, 577 007, Karnataka, India; [2]Department of Studies in Food Technology, Davangere University, Davangere, 577 007, Karnataka, India; [3]Department of Biotechnology and Bioinformatics, School of Life Sciences, JSS Academy of Higher Education and Research, Mysuru, Karnataka, 570 015, India; [4]Department of Metallurgy and Materials Engineering, Malawi Institute of Technology, Malawi University of Science and Technology, Limbe, Malawi; [5]Department of Epidemic Disease Research, Institute for Research and Medical Consultations (IRMC), Imam Abdulrahman Bin Faisal University, Dammam, 31441, Saudi Arabia; [6]National Centre for Biotechnology, King Abdulaziz City for Science and Technology (KACST), Riyadh, 11442, Saudi Arabia; [7]Laboratory Medicine Department, Faculty of Applied Medical Sciences, Umm Al-Qura University, Makkah, 24231, Saudi Arabia; [8]Department of Clinical Laboratory Sciences, College of Applied Medical Sciences, Taif University, Taif, 21944, Saudi Arabia; [9]Department of Studies in Botany, Anjuman Arts, Science and Commerce College, Vijayapura, Karnataka, 586 101, India; [10]Department of Studies in Botany, Davangere University, Davangere, 577 007, Karnataka, India; [11]Department of Sciences, Amrita School of Arts and Sciences, Amrita Vishwa Vidyapeetham, Mysuru Campus, Mysuru, Karnataka, 570 026, India; [12]School of Agriculture, Geography, Environment, Ocean and Natural Sciences (SAGEONS), The University of the South Pacific, Suva, Fiji

*These authors contributed equally to this work

Correspondence: Shiva Prasad Kollur; Siddappa B Kakkalameli, Email shivachemist@gmail.com; dubotsiddu@gmail.com

Introduction: Cancer disease is known due to its unregulated proliferation of cells that have evolved from the body's regular cells. The disease develops as a result of epigenetic and genetic modifications, tumor suppressor gene inactivation, and oncogene activation. The present work describes an environmentally benign approach for the synthesis of manganese oxide nanoparticles (MnO_2 NPs) using *Gmelina arborea* fruit extract (GAE) in an aqueous medium.

Methods: The study evaluated the formation of MnO_2 NPs and their anticancer efficacy against MCF-7 breast cancer cell line.

Results: The formation of MnO_2 NPs was confirmed through powder X-ray diffractometer (XRD), scanning electron microscopy (SEM), transmission electron microscopy (TEM) and high-resolution transmission electron microscopy (HR-TEM). The crystalline nature of as-prepared MnO_2 NPs was evident from XRD pattern. The morphology of the material was studied using SEM analysis, which suggested a rod-like nature with an average diameter of 50 nm. Further, the TEM and HR-TEM images confirmed the rod shape of the as-prepared MnO2 NPs with an interplanar distance of 0.271 nm. In addition, the concentric rings from selected area electron diffraction (SAED) analysis show the crystalline nature of the as-prepared material, which further supports the obtained XRD pattern. The anticancer efficacy of MnO_2 NPs was evaluated against MCF-7 breast cancer cell line, which showed up to 96% inhibition of the cells at 400 µg/mL concentration.

Conclusion: Bio-conjugation of MnO_2 NPs can provide enough scope for the therapeutic use of *Gmelina arborea*, assuming appropriate mechanistic evaluations are conducted.

Keywords: *Gmelina arborea*, MnO_2 NPs, HR-TEM, MCF-7

Introduction

Cancer disease is known for its unregulated proliferation of cells that have evolved from the body's regular cells. The disease develops as a result of epigenetic and genetic modifications, tumor suppressor gene inactivation, and oncogene activation.[1] In developing countries, it has become of the leading causes of death. The MTT assay uses live cells to assess in vitro mammalian cellular development, survival, proliferation and even the cytotoxic potential of different compounds

Received: 15 September 2021
Accepted: 24 January 2022
Published: 25 February 2022

can be evaluated using this assay.[2] The percentage of viable cells in a cell suspension is determined using cell viability assays.[3] Membrane integrity has remained the most common metric for determination of cell viability.[4]

Since ancient times, *Gmelina arborea (G. arborea)* belonging to Verbenaceae family has been used in traditional medicinal practices such as Ayurveda.[5] It is a tree that grows in Asia's moist deciduous forests and was introduced to Africa and South America as a plantation tree species mainly for its timber-yielding qualities.[6] The tree's medicinal properties are also highly regarded. Almost every portion of the tree is used as medicine to treat fevers, skin issues and stomach problems. Flavonoids, iridoid glycosides, and lignans are among the phytochemical constituents present in this plant.[7] All the organs of this plant have known medicinal value, and have been used for a long time as antimicrobial, anti-diabetic, anthelmintic, hepatoprotective, anti-aging, antiepileptic, analgesic and diuretic agents.[8] As a thriving interdisciplinary field of exploration in an assortment of fields, nanotechnology can empower inventive applications in farming, like pesticide conveyance, nano-sensors, pesticide debasement, micro-nutrients for effective use, etc. A few inorganic and natural metal oxide nanomaterials, just as a few crossbreed nanomaterials, are progressively being utilized as elective antibacterial specialists in biomedical applications because of their strange uncommon nano-size structure, high surface-to-volume proportion and unrivaled physicochemical properties' attributes.[9] MnO_2 NPs are non-toxic in nature that is relatively simple to obtain when compared to other different inorganic metal oxides.[10] Recent advancements have resulted in notable improvements in materials and drugs, all of which have tremendous potential.[11]

Based on all the above-mentioned facts in the present investigation, the MnO_2 NPs are synthesized from GAE and were characterized using XRD, SEM, TEM and HRTEM techniques. Further, as-prepared MnO_2 NPs were screened for its tumoricidal effect against MCF-7 breast cancer cell line.

Materials and Methods

The precursor, manganese acetate tetrahydrate [$Mn(OAc)_2.4H_2O$] was obtained from Loba chemicals (Bangalore, India). Demineralized water was collected from an ELGA RO system and was used throughout the experiments (Elga Veolia, Lane End, UK). The crystalline phases were recorded on Bruker X-ray diffractometer with a scan range of 20–80° at a 2°/min scan rate using Cu Kα (1.5406 Å) radiation (Bruker, Karlsruhe, Germany). The morphology and elemental composition were studied using scanning electron microscopy (SEM) and énergy dispersive X-ray (EDX) mapping, respectively, which were recorded on a Zeiss microscope (Carl Zeiss, White Plains, NY, USA). Transmission electron microscopy (TEM) images and Selected Area Electron Diffraction (SAED) patterns were recorded on a JEOL 2100F FEG apparatus operating at 200 kV after casting a drop of MnO2 NPs for dispersion in ethanol over a Cu grid (Jeol, Akishima, Tokyo, Japan). Breast cancer cells (MCF-7) were procured from the ATCC and cultured in Dulbecco's Modified Eagle Medium (DMEM) with 10% fetal bovine serum (FBS), penicillin (100 IU/mL), and streptomycin (100 µg/mL) in 5% CO2 at 37°C until confluence.

Collection and Preparation of *Gmelina arborea* Fruit Extract

Dr Chandrashekar S performed the unambiguous authentication of the specimen that was then deposited in the herbarium with the voucher specimen number GA01 in the Department of Biotechnology and Bioinformatics, JSS AHER, Mysore, Karnataka, India. The plant material was available in the University campus, the proper guidance was taken from the botanist while collecting the plant materials for the study. The fertile fruits of G. arborea were collected from the tropical forest of Malnad region in Karnataka, India. The collected plant material was surface sterilized 2–3 times with running tap water to remove adhered dust impurities followed by sterile double-distilled water and then air-dried at room temperature for 3–4 days. The yellow fruits were washed several times with demineralized water, sun-dried, finely ground, and 10% aqueous extracts were made as follows: Using a mortar and pestle, 1 gram of powder was mixed with 10 mL of water and thoroughly homogenized. The suspension was then centrifuged at 4°C for 15 minutes at 10,000 rpm. The supernatant was collected and stored in aliquots at a 20°C.[12]

Synthesis of MnO_2 NPs from *Gmelina arborea* Fruit Extract

The MnO_2 NPs were synthesized by reacting aqueous solution of manganese acetate (2 mm) with aqueous extract of *G. arborea fruit* (0.65 g) in 15 mL of deionized water. The above reaction mixture was stirred for 2.5 h at room temperature. The color change was observed from colorless to reddish brown, which primarily indicated the formation of MnO_2 NPs via metal reduction. Upon allowing the above solution to age for 24 h, a black product indicating the complete stabilization of MnO_2 NPs was obtained. The resulting product was centrifuged, filtered off, washed thrice with absolute ethanol and then with acetone to obtain pure MnO_2 NPs. The obtained powder was dried at 80 °C for 6 h and used for further studies.

Measurement of Cell Viability Using MTT Assay

The cells were seeded in a 96-well flat-bottom microplate and held overnight at 37°C, 95% humidity, and 5% CO_2. The samples were treated at various concentrations of GAE and MnO_2 NPs (12.5, 25, 50, 100, 200 and 400 µg/mL). For another 24 h, the cells were incubated. The wells were washed twice with PBS before being filled with 20 µL of MTT staining solution and incubated at 37°C. After 4 h, 100 µL DMSO was applied to each well to dissolve the formazan crystals, and absorbance was measured at 570 nm using a microplate reader using the below-given formula.[13]

$$\text{Surviving cells (\%)} = \text{Mean OD of test compound}/\text{Mean OD of Negative control} \times 100$$

Results and Discussion

XRD (X-Ray Diffraction) Analysis

The XRD pattern of as-prepared MnO_2 NPs is shown in Figure 1. The crystalline phases of MnO_2 NPs revealed diffraction peaks at 2θ = 12.8°, 19.1°, 27.3°, 33.1°, 49.2°, 54.8°, and 68.2° corresponding to (110), (200), (310), (201),

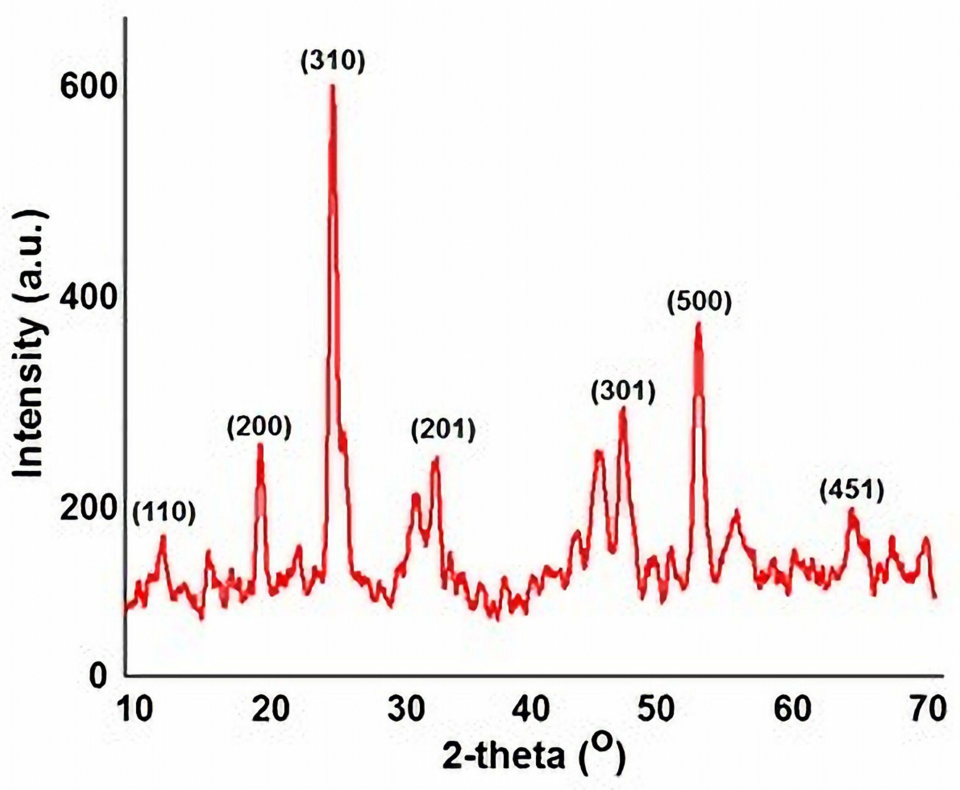

Figure 1 Powder X-ray diffraction pattern showing the crystalline planes of as-prepared MnO_2 NPs.

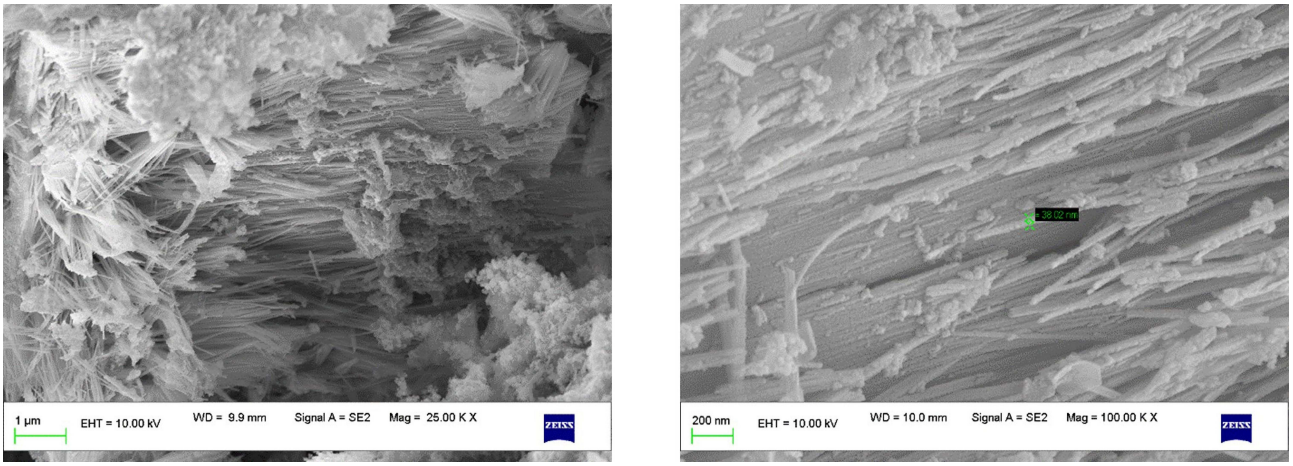

Figure 2 SEM images of as-prepared MnO_2 NPs in different magnifications.

(301), (500) and (451) crystal planes. This further depicts the cubic structure of the as-obtained material with lattice parameter a = 4.46 Å. The indexed crystalline planes were in good agreement with the standard values JCPDS card PDF file no. 44–0141, further confirmed the crystalline nature of MnO_2.[14]

SEM (Scanning Electron Microscopy) Analysis

The morphology of as-prepared MnO_2 NPs revealed that it is composed of nanorods with an average size ranging between 50 and 60 nm. It is seen from Figure 2 that the MnO_2 NPs comprise the dense cloud and cluttered nanorods. Further, it can be seen from the magnified SEM image that the as-prepared MnO_2 NPs microenvironment consists of furrowed nanorods. Furthermore, the EDX analysis of MnO_2 NPs affirmed that the ratio of Mn:O as 1:2 (Figure 3). The uniform distribution of Mn and O are seen from the elemental mapping image. The intensity of oxygen particles was observed to be higher than that of Mn particles.[15,16]

TEM (Transmission Electron Microscopy) Analysis

Transmission scanning electron microscopy (TEM) images of as-prepared MnO_2 NPs are depicted in Figure 4. The average sizes of the MnO_2 NPs are between 40 and 50 nm. The rod-shaped nature of MnO_2 NPs for the sample is evident from the TEM image. Moreover, the aggregate blocks with the porous structure of as-prepared MnO_2 NPs are seen from

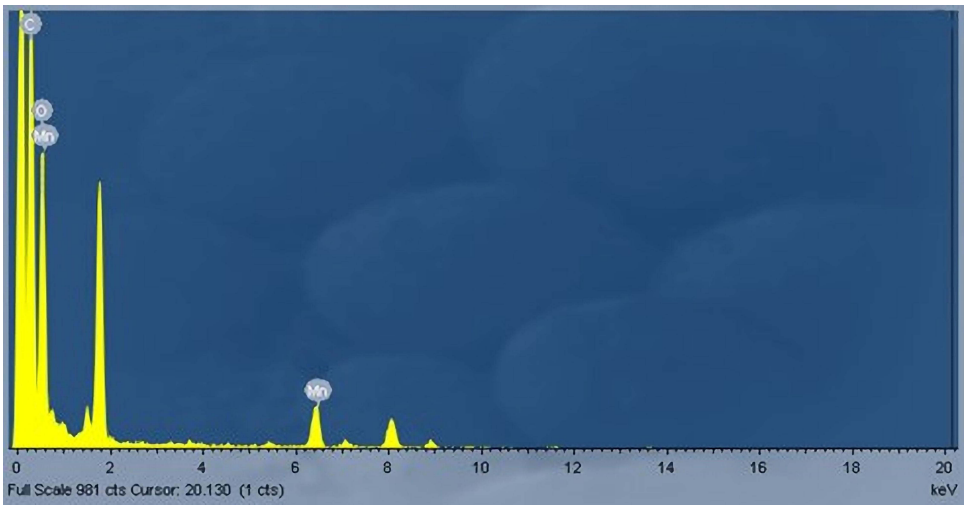

Figure 3 Energy-dispersive X-ray (EDX) spectra of as-prepared MnO_2 NPs.

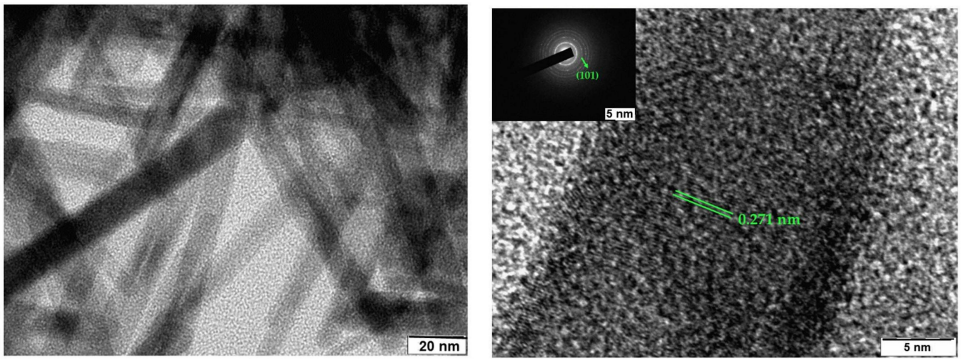

Figure 4 TEM (left) and HR-TEM (right) micrographs with SAED patterns (inset) of as-prepared MnO_2 NPs.

TEM image. Further, the HR-TEM image of as-prepared MnO_2 NPs revealed that the interplanar spacing between two lattice fringes was 0.271 nm, corresponding to (101) lattice plane of MnO_2 NPs. Furthermore, SAED pattern affirms the crystalline structure of as-prepared MnO_2 NPs.

Cytotoxicity Effect of MnO_2 NPs Against MCF-7 Breast Cancer Cell Line

Both GAE and MnO_2 NPs exhibited dose-dependent cytotoxicity on breast adenocarcinoma MCF-7 cell lines. However, the GAE coated with MnO_2 NPs significantly showed better activity with respect to GAE alone (Figure 5). The cells were treated in hypoxic conditions for 24 h, with differential groupings of the tests going from 12.5, 25, 50, 100, 200 and 400 μg/mL. Moreover, the nanoparticle conveyance of GAE was found to reduce the dose required to inhibit the in vitro MCF-7 cell growth. The highest observed activity of GAE was 46% inhibition of MCF-7 cells at 400 μg/mL, while the

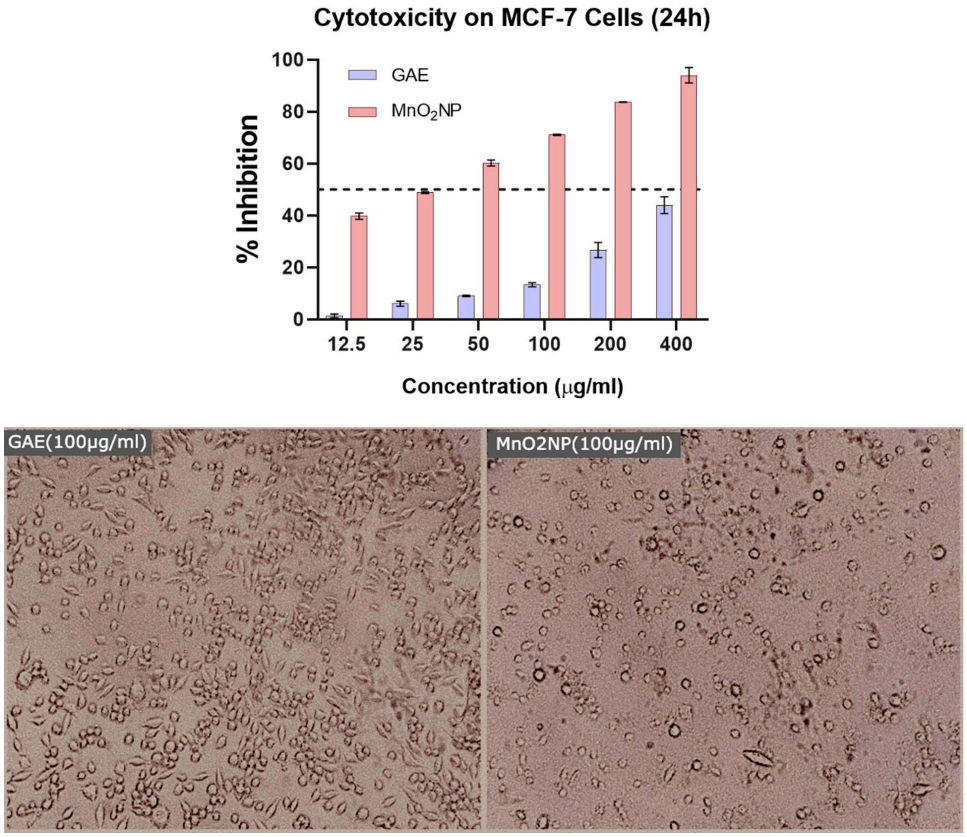

Figure 5 Cytotoxicity of as-prepared MnO_2 NPs against MCF-7 cells (top). Photomicrographs of MCF-7 cells treated with GAE (100 μg/mL) and MnO_2 NPs (100 μg/mL).

MnO_2 NPs inhibited up to 96% of the cells. Thereby implying that MnO_2 NPs guided conveyance of *G. arborea* improves its antitumor action.[17] Additionally, the treatment of MCF-7 cells with the GAE coated MnO_2 NPs changed the cellular morphology to rounded, thereby indicating the normalization of cells.[18,19]

Conclusions and Future Perspectives

In conclusion, MnO_2 NPs from *Gmelina arborea*, a medicinally important plant (fruit extract) were successfully generated. The HRTEM analysis was used to determine spherical morphology and scale of freshly collected MnO_2 NPs. The tentative efficacy of the MnO_2 NPs as tumoricidal and antibacterial agents was carried out to confirm the bioactivities of MnO_2 NPs were found to be substantially enhanced when they were bio-conjugated with GAE. Furthermore, bio-conjugation of MnO_2 NPs can provide enough scope for the therapeutic use of *Gmelina arborea*, assuming appropriate mechanistic evaluations are conducted. Comprehensive evaluation of safety is an urgent problem for the clinical application of nanomaterials. Although MnO_2 nanoparticles have excellent performance for enhanced cancer therapy, the detailed toxicity profiles and metabolic mechanism of MnO_2-based nanomaterials should be further evaluated to ensure their future safe clinical applications. Improving the selectivity and specificity of MnO_2-based nanoplatforms in cancer therapy will be another challenge in the future. Furthermore, in addition to the mostly explored tumor theranostics, these MnO_2-based nanoplatforms are expected to have more applications in other biomedical fields, such as tissue engineering, anti-bacterial, diabetes, and even cardiovascular diseases. Those research directions, however, require further in-depth studies.

Acknowledgments

The authors thank the Director, Indian Institute of Science, Bengaluru for analytical facilities. SPK is grateful to the Director, Amrita Vishwa Vidyapeetham, Mysuru campus for infrastructure facility. SP, SKP and CS acknowledge the facility and infrastructure provided by the JSS Academy of Higher Education and Research (JSSAHER), Mysuru, India. The authors would like to thank Taif University, Taif, Saudi Arabia, for their support (Taif University Researchers Supporting Project number: TURSP-2020/80), Taif University, Taif, Saudi Arabia. The authors are grateful to the financial assistance from DUSMYTR-GRANT SANCTION LETTER; No;DU/HRM/2020-21/6045/Dated: 03-03-2021 Davangere University, Davangere, Karnataka India and Authors acknowledge the support and infrastructure provided by the Davangere University, Davangere, Karnataka, India.

Disclosure

The authors declare that there are no conflicts of interest.

References

1. Zhu X, Liu Y, Yuan G, et al. In situ fabrication of MS@MnO2 hybrid as nanozymes for enhancing ROS-mediated breast cancer therapy. *Nanoscale*. 2020;12(43):22317–22329. doi:10.1039/D0NR03931D
2. Sun P, Deng Q, Kang L, Sun Y, Ren J, Qu X. A smart nanoparticle-laden and remote-controlled self-destructive macrophage for enhanced chemo/chemodynamic synergistic therapy. *ACS Nano*. 2020;14(10):13894–13904. doi:10.1021/acsnano.0c06290
3. Sharma GN, Dave R, Sanadya J, Sharma P, Sharma KK. Various types and management of breast cancer: an overview. *J Adv Pharm Technol Res*. 2010;1(2):109–126.
4. Peng L, Xu T, Long T, Zuo H. Association between BRCA status and P53 status in breast cancer: a meta-analysis. *Med Sci Monit*. 2016;22:1939–1945.
5. Chen WY. Patient education: factors that modify breast cancer risk in women (Beyond the Basics); 2015. Available from: http://www.uptodate.com/contents/factors-that-modify-breast-cancer-risk-in-women-beyond-the-basics. Accessed January 25, 2022.
6. Sahu A, Kwon I, Tae G. Improving cancer therapy through the nanomaterials-assisted alleviation of hypoxia. *Biomaterials*. 2020;228:119578. doi:10.1016/j.biomaterials.2019.119578
7. Liu Y, Guo J, Huang L. Modulation of tumor microenvironment for immunotherapy: focus on nanomaterial-based strategies. *Theranostics*. 2020;10(7):3099–3117. doi:10.7150/thno.42998
8. Liu X, Hao Y, Popovtzer R, Feng L, Liu Z. Construction of enzyme nanoreactors to enable tumor microenvironment modulation and enhanced cancer treatment. *Adv Healthcare Mater*. 2020;10:2001167. doi:10.1002/adhm.202001167
9. Gao F, Tang Y, Liu WL, et al. Intra/extracellular lactic acid exhaustion for synergistic metabolic therapy and immunotherapy of tumors. *Adv Mater*. 2019;31(51):1904639. doi:10.1002/adma.201904639
10. Kollur SP, Alakananda P. Green synthesis of MnO_2 nanorods using *Phyllanthus amarus* plant extract and their fluorescence studies. *Green Process Synth*. 2017;6:549–554.

11. Korrat A, Greiner T, Maurer M, Metz M, Fiebig HH. Gene signature-based prediction of tumor response to cyclophosphamide. *Cancer Genomics Proteomics*. 2007;4(3):187–195.
12. Essien ER, Atasie VN, Oyebanji TO, Nwude DO. Biomimetic synthesis of magnesium oxide nanoparticles using Chromolaena odorata (L.) leaf extract. *Chem Pap*. 2020;74(7):2101–2109. doi:10.1007/s11696-020-01056-x
13. Abdallah Y, Ogunyemi SO, Abdelazez A, et al. The green synthesis of MgO nano-flowers using Rosmarinus officinalis L. (Rosemary) and the antibacterial activities against Xanthomonas oryzae pv. oryzae. *Biomed Res Int*. 2019;1–8. doi:10.1155/2019/5620989
14. Wang JW, Chen Y, Chen BZ. A synthesis method of MnO_2/activated carbon composite for electrochemical supercapacitors. *J Electrochem Soc*. 2015;162:1654–1661. doi:10.1149/2.0031509jes
15. Nguta JM, Appiah-Opong R, Nyarko AK, et al. In vitro antimycobacterial and cytotoxic data on medicinal plants used to treat tuberculosis. *Data Brief*. 2016;7:1124–1130. doi:10.1016/j.dib.2016.03.088
16. Kumbar VM, Peram MR, Kugaji MS, et al. Effect of curcumin on growth, biofilm formation and virulence factor gene expression of Porphyromonas gingivalis. *Odontology*. 2021;109(1):18–28. doi:10.1007/s10266-020-00514-y
17. Shiva PK, Shashanka KP, Ravindra V, et al. Antitumor potential of green synthesized ZnONPs using root extract of withania somnifera against human breast cancer cell line. *Separations*. 2021;8(1):8. doi:10.3390/separations8010008
18. Shiva PK, Shashanka KP, Sushma P, et al. Luteolin-fabricated ZnO nanostructures showed PLK-1 mediated anti-breast cancer activity. *Biomolecules*. 2021;11(3):385. doi:10.3390/biom11030385
19. Shashanka KP, Prashanth MV, Pushkal SR, Suma MN, Devananda D, Subbarao VM. Phytochemical fractions from annona muricata seeds and fruit pulp inhibited the growth of breast cancer cells through cell cycle arrest at G0/G1 phase. *J Cancer Res Ther*. 2020;16:1235–1249. doi:10.4103/jcrt.JCRT_494_19